Molecular & Biochemical Parasitology 193 (2014) 55–65

Contents lists available at ScienceDirect

Molecular & Biochemical Parasitology

Comparative analysis of respiratory chain and oxidative phosphorylation in *Leishmania tarentolae*, *Crithidia fasciculata*, *Phytomonas serpens* and procyclic stage of *Trypanosoma brucei*

Zdeněk Verner[a,b], Petra Čermáková[a], Ingrid Škodová[a,b], Bianka Kováčová[a], Julius Lukeš[b,c], Anton Horváth[a,*]

[a] Department of Biochemistry, Faculty of Natural Sciences, Comenius University, Bratislava, Slovakia
[b] Biology Centre, Institute of Parasitology, České Budějovice (Budweis), Czech Republic
[c] Faculty of Sciences, University of South Bohemia, České Budějovice (Budweis) , Czech Republic

ARTICLE INFO

Article history:
Received 13 November 2013
Received in revised form 5 February 2014
Accepted 6 February 2014
Available online 17 February 2014

Keywords:
Mitochondrion
Oxidative phosphorylation
Trypanosoma
Leishmania
Phytomonas
Crithidia

ABSTRACT

Trypanosomatids are unicellular parasites living in a wide range of host environments, which to large extent shaped their mitochondrial energy metabolism, resulting in quite large differences even among closely related flagellates. In a comparative manner, we analyzed the activities and composition of mitochondrial respiratory complexes in four species (*Leishmania tarentolae*, *Crithidia fasciculata*, *Phytomonas serpens* and *Trypanosoma brucei*), which represent the main model trypanosomatids. Moreover, we measured the activity of mitochondrial glycerol-3-phosphate dehydrogenase, the overall oxygen consumption and the mitochondrial membrane potential in each species. The comparative analysis suggests an inverse relationship between the activities of respiratory complexes I and II, as well as the overall activity of the canonical complexes and glycerol-3-phosphate dehydrogenase. Our comparative analysis shows that mitochondrial functions are highly variable in these versatile parasites

1. Introduction

Trypanosomatida is a species-rich group of protists parasitizing a wide variety of hosts. It belongs to the class Kinetoplastea characterized by a number of unique molecular features. In the traditional, morphology-based system Trypanosomatida comprises of several monoxenous (=single host) and dixenous (=two-host) genera. Recent extensive re-evaluation of the group using molecular data identified 12 main clades that do not support the monophyly of most traditional genera [1], leading to the description of new ones based on molecular characteristics [2,3]. For comparative analysis of respiratory chain we chose members of the genera *Leishmania*, *Crithidia*, *Phytomonas* and *Trypanosoma*, each represented by a well-studied species, briefly introduced below.

Trypanosoma brucei is a causative agent of African human sleeping sickness and nagana of livestock. Upon ingestion of a blood meal from an infected mammal, the flagellates establish themselves in a tse-tse fly vector (*Glossina* spp.). In its gut, the short-stumpy form transforms into the dividing procyclic cells, which migrate into the salivary glands and evolve into the infectious metacyclic stage, ready to be injected into the bloodstream of another mammalian host [4]. *Leishmania tarentolae* is an intracellular parasite of white blood cells of a Moorish gecko (*Tarentola mauritanica*) [5] that uses a sandfly (*Phlebotomus* sp.) as its vector. Within the vertebrate host, the parasite proliferates in the form of flagellum-lacking amastigotes, which upon rupture of the host cell infect new macrophages. In the gut of the sandfly, the amastigote transforms via procyclic promastigote into non-dividing metacyclic promastigote, which close the cycle by becoming again infectious for vertebrates [6]. *Phytomonas serpens* is along with other members of the genus *Phytomonas* an economically important parasite of the phloem sap, latex and/or fruits of various plants, including coconut and oil palms and coffee tree [7]. This flagellate is transmitted from one plant

Abbreviations: ACA, aminocaproic acid; BHI, brain heart infusion; CoQ, coenzyme Q; DBH, 2,3-dimethoxy-5-methyl-6-dodecyl-1,4-benzoquinol; DCIP, 2,6-dichlorophenolindophenol; DPI, diphenyl iodonium; FBS, fetal bovine serum; FCCP, carbonyl cyanide 4-(trifluoromethoxy) phenylhydrazone; mtG3PDH, mitochondrial FAD-dependent glycerol-3-phosphate dehydrogenase; NTB, nitrotetrazolium blue; OXPHOS, oxidative phosphorylation; PE, phycoerythrin; Q2, ubiquinon-2; RC, respiratory chain; SHAM, salicylhydroxamic acid; TAO, trypanosomal alternative oxidase; TMRE, tetramethylrhodamide ethyl ester perchlorate.

* Corresponding author.
E-mail address: horvath@fns.uniba.sk (A. Horváth).

http://dx.doi.org/10.1016/j.molbiopara.2014.02.003
0166-6851/

to another by various true bugs (Heteroptera), where it occurs in the form of a promastigote, which is also the stage maintained in the culture and analyzed below. Finally, the monoxenous flagellates are represented by *Crithidia fasciculata* known to infect the gut of mosquitoes (*Culex* spp.). In this host, it occurs either as a motile form called nectomonad, propagated in the culture, or as an immotile form, attached to the host tissues, which is known as haptomonad [8]. The parasite is mostly transmitted by infected faeces but probably also by other means [1].

Canonical respiratory chain (RC) of eukaryotes consists of four different multi-subunit enzymes called respiratory complexes I–IV residing in the mitochondrial inner membrane. The complexes transmit electrons from reduced co-factors, produced by catabolic pathways, to their final acceptor oxygen. Three complexes (I, III and IV) use the energy of transferred electrons to produce proton gradient across the mitochondrial inner membrane. Complex V typically utilizes the produced proton gradient to form ATP and along with RC constitutes the oxidative phosphorylation (OXPHOS) machinery.

Complex I (NADH:ubiquinone oxidoreductase; EC 1.6.5.3) is a proton pump transferring electrons from a reduced nicotine amide dinucleotide (NADH) to ubiquinone, regenerating NAD^+ and trafficking protons from matrix into the inter-membrane space. Catalytic part of the complex contains seven iron-sulfur clusters and a flavine mononucleotide as cofactors [9]. Complex II (succinate:ubiquinone oxidoreductase; EC 1.3.5.1) is an enzymatic complex that directly couples Krebs cycle with RC and possesses covalently-bound flavine adenine dinucleotide as well as heme b [10]. It is also the smallest respiratory complex of the respiratory chain. Complexes I and II donate electrons to a lipophilic compound known as ubiquinol or coenzyme Q (CoQ) oxidizing it to ubiquinone. In a canonical respiratory chain, CoQ is reduced by complex III (ubiquinone:cytochrome *c* oxidoreductase; EC 1.10.2.2), which in a typical respiratory chain operates as the second proton pump, the subunits of which also contains co-factors, such as heme and Fe–S clusters [11]. Energy for pumping is derived from electrons passing through the complex via the so-called Q-cycle to a soluble cytochrome *c* located in the inter-membrane space [12]. The last RC enzyme is complex IV (cytochrome *c* oxidase; EC 1.9.3.1), which transfers electrons to oxygen, an action coupled with proton pumping [13]. Complex V (F_1F_O-ATP synthase; EC 3.6.3.14), final component of the oxidative phosphorylation in eukaryotes, channels protons from the inter-membrane space back to the mitochondrial matrix. Energy of this flow is used for synthesizing ATP from phosphate and ADP [14].

All four model trypanosomatids were already studied in the past in respect to their mitochondrial metabolism in general and oxidative phosphorylation in particular. However, the data were obtained in different laboratories using various techniques available at the time, and it is rather difficult to compare them in order to get an insight into the variability of mitochondrial physiology of trypanosomatids. Therefore, we set to compare side-by-side features of RC and OXPHOS of the four representative trypanosomatids, which allowed us to reveal differences in their overall mitochondrial physiology. We believe that this study deepens our understanding of the mitochondrial bioenergetics of the Trypanosomatida.

2. Materials and methods

2.1. Cultivation

T. brucei (strain 29–13) was cultivated in regular SDM-79 supplemented with 10% (v/v) heat-inactivated FBS as described previously [15]. *L. tarentolae* (strain UC), *P. serpens* (strain 9T) and *C. fasciculata* (strain UC) were grown in BHI medium supplemented with hemin [16,17]. Cultures were kept at 27 °C and diluted 10× upon reaching 1×10^7/mL for *T. brucei* and 5×10^7/mL for the other species.

2.2. Mitochondrial isolation

Mitochondrion-enriched fraction was obtained as described previously [18]. Briefly, 10^9 cells were harvested by spinning at 1000 g for 10 min at room temperature, the pellet was resuspended in STE buffer (250 mM sucrose, 20 mM Tris–HCl pH 7.9, 2 mM EDTA), and the cells were spun at maximum *g* for 10 min at 4 °C. All subsequent steps were performed at 4 °C. The pellet was dissolved in 1.5 mL pre-cooled NET buffer (150 mM NaCl, 100 mM EDTA, 10 mM Tris–HCl pH 8) and left standing on ice for 10 min, spun again at maximum *g* for 10 min and the supernatant was removed. The pellet was dissolved in 1 ml DTE buffer (1 mM Tris–HCl pH 7.9, 1 mM EDTA) and passed through a G25 needle into a new tube containing 120 μl 60% sucrose. Following a 10 min spin at maximum g and careful removal of the supernatant, the pellet was dissolved in 500 μl STM buffer (250 mM sucrose, 20 mM Tris–HCl pH 7.9, 2 mM $MgCl_2$) with 10 U of DNase I and incubated for 30 min on ice. The reaction was stopped by the addition of 500 μl STE buffer. The pellet obtained after another spin was washed twice with STE and the isolated mitochondrial fraction was kept at −80 °C until use. The lysate was prepared by resuspending mitochondria in 0.5 M aminocaproic acid and dodecyl maltoside to the final concentration of 2% and the lysis was performed for 30 min on ice. Upon incubation, the lysate was spun for 30 min at maximum *g* at 4 °C and both pellet and supernatant were used.

2.3. Enzymatic assays

NADH dehydrogenase (complex I/NDH2) was measured as previously described [19]. Briefly, in 1 ml of NDH buffer (50 mM KPi, pH 7.5; 1 mM EDTA, pH 8.5; 0.2 mM KCN). Five μl of mitochondrial lysate and 5 μl of 20 mM NADH were mixed with the buffer and the reaction was started by the addition of 10 μl of either 2 mM coenzyme Q_2 or 5 mM potassium ferricyanide. The reaction was followed at 340 nm for 3 min.

Succinate dehydrogenase (complex II) was measured as previously described [20]. Briefly, five μl of the mitochondrial lysate was added to the 1 ml of SDH buffer (25 mM KPi, pH 7.2; 5 mM $MgCl_2$; 20 mM sodium succinate), mixed and incubated in 30 °C for 10 min. Next, antimycin A, rotenone, KCN and 2,6-dichlorophenolindophenol were separately added to a final concentration of 2 μg/ml, 2 μg/ml, 2 mM and 50 μM, respectively. Upon mixing, the background reactions were monitored at 600 nm. The reaction itself was started upon the addition of coenzyme Q_2 to a final concentration of 65 μM, and was followed at 600 nm for 5 min.

Activities of complexes III and IV were measured as previously described [21]. Cytochrome *c* reductase (complex III) was measured in 1 ml of QCR buffer (40 mM NaPi, pH 7.4; 0.5 mM EDTA, pH 8.5; 20 mM sodium malonate; 50 μM cytochrome *c*; 0.005% [w/v] dodecyl maltoside). Simultaneously, 2 μl of the mitochondrial lysate and 2 μl of 2,3-dimethoxy-5-methyl-6-dodecyl-1,4-benzoquinol (DBH) were added and the reaction was monitored at 550 nm for 1 min. DBH was prepared by reduction of decylubiquinon as described elsewhere [22]. Cytochrome *c* oxidase (complex IV) was measured in 1 ml of COX buffer (40 mM NaPi, pH 7.4; 0.5 mM EDTA, pH 8.5; 20 μM cytochrome *c*; 30 μM ascorbic acid; 0.005% [w/v] dodecyl maltoside; solution was allowed to stand overnight to oxidize surplus of ascorbic acid). Ten μl of the mitochondrial lysate was added to the buffer and the reaction was monitored at 550 nm for 10 min.

ATP-hydrolase (complex V) was measured as previously described [23]. Briefly, in 1 ml of TC buffer (200 mM KCl; 10 mM Tris–HCl, pH 8.2; 2 mM $MgCl_2$) using 1 mg of the mitochondrial proteins. The reaction was started by the addition of ATP to a final concentration of 5 mM. After 5 and 10 min, respectively, 95 μl of the mixture was transferred into a new tubes containing 5 μl of 3 M trichloracetic acid. The mixture was incubated on ice for 30 min, and then spun at 16,000 × *g* for 10 min at 4 °C. One ml of the Sumner reagent (8.8% [w/v] $FeSO_4 \times 7\ H_2O$; 375 mM H_2SO_4; 6.6% [w/v] $(NH_4)6Mo_7O_{24} \times 4\ H_2O$) was mixed with 90 μl of the supernatant and incubated at room temperature for 15 min, the absorbance being measured at 610 nm.

FAD-dependent G3PDH activity was measured as described recently [24]. Briefly, in 1 ml of the G3PDH buffer (50 mM Tris–HCl, pH 7.0; 0.075 mM 2,6-dichlorophenolindophenol and 0.1 mM phenazine methosulfate) using 75 μg of the mitochondrial lysate. The activity was measured by recording the decrease of absorbance at 600 nm triggered by the addition of 50 mM DL-glycerol-3-phosphate.

2.4. In-gel staining of respiratory complexes

For activity staining, mitochondrial lysate was loaded on a 2–15% gradient PAGE gel and run either under blue-native (BN) [25] or high resolution clear-native (hrCN) [26] conditions. Loading buffer (1×) for BN-PAGE contained 0.5 M aminocapronic acid (ACA) and 5% (w/v) Coomassie brilliant blue G-250; 10× cathode buffer contained 0.5 M Tricine, 75 mM imidazol-HCl, pH 7.0 and 0.02% (w/v) Coomassie brilliant blue G-250; 10× anode buffer contained 0.25 M imidazol, pH 7.0. Fifty to 100 μg proteins were lysed in 20 μl of 0.5 M ACA and 2% dodecyl maltoside as described in Section 2.2. Then, 1.5 μl of loading buffer was added and the mixture was incubated on ice for 10 min. Next, the mixture was loaded onto a gel and run with a limit of 1.5 W in 4 °C. For CN-PAGE, 5× loading buffer contained 1% Ponceau S dissolved in 50% (v/v) glycerol; 1× cathode buffer contained 0.01% dodecyl maltoside, 5 mM Tricine, 7.5 mM imidazol, pH 7.0 and 0.05% (w/v) deoxycholate; 10× anode buffer contained 0.25 M imidazol-HCl, pH 7.0. Samples were prepared as for BN with the exception of the cathode buffer being used instead of ACA.

Activities of complexes I, II, IV and V were detected by techniques adapted from [27]. Complex I activity was visualized after BN-PAGE using 100 mM Tris–HCl, pH 7.4, with 140 μM NADH (Fluka) and 1 mg/ml nitrotetrazolium blue (Fluka). The staining took place overnight in dark at room temperature. Complex II activity was visualized after hrCN-PAGE using 50 mM sodium phosphate buffer, pH 7.4, containing 84 mM sodium succinate, 0.2 mM phenazine methosulfate, 4.5 mM EDTA, pH 8.5, 10 mM KCN and 2 mg/mg nitrotetrazolium blue. The reaction took place in for 3 hrs dark at room temperature. Putative complex III activity was visualized after hrCN-PAGE using method developed by Wittig et al. [28]. The gel was stained by 1 mg/ml diamino benzidine in 50 mM sodium phosphate buffer, pH 7.2 for 4 h. Complex IV was stained upon BN-PAGE using 50 mM sodium phosphate buffer, pH 7.4, containing 1 mg/ml diamino benzidine, 24 U/ml catalase, 1 mg/ml cytochrome *c* and 75 mg/ml sucrose. Staining took place overnight at room temperature. Finally, complex V was visualized upon BN-PAGE using 35 mM Tris containing 270 mM glycine, 19 mM $MgSO_4$, 0.3% (w/v) $Pb(NO_3)_2$ and 11 mM ATP. Staining took place overnight at room temperature.

2.5. Western blot analysis

Proteins obtained upon mitochondrial lysis were resolved either on a native or denaturing polyacrylamide gels and blotted onto a nitrocellulose membrane. The membrane was blocked using either 5% milk or 3% BSA (both in TBS buffer [50 mM Tris–HCl, pH 8.0; 150 mM NaCl, 0.05% {v/v} Tween 20]) overnight. Upon blocking, the membrane was immunodecorated using the following antibodies: complex I – monoclonal anti-39 kDa subunit of the bovine complex [29] (dilution 1:250); complex II – polyclonal anti-SDH66 raised against an oligopeptide derived from a trypanosomal protein [30] (dilution 1:1000); complex III – monoclonal anti-Rieske trypanosomal protein [18] (dilution 1:500) and polyclonal anti-apocytochrome c_1 trypanosomal protein [18] (dilution 1:500); complex IV – polyclonal anti-trCOIV leishmanial protein [31] (dilution 1:500) and polyclonal anti-coxVI trypanosomal protein [18] (dilution 1:500); complex V – polyclonal anti-beta subunit of crithidial F_1 moiety [17] (dilution 1:1000) and polyclonal anti-p18 trypanosomal protein (kindly provided by L. Simpson; raised in rabbit; dilution 1:2000); loading control was performed using polyclonal anti-gGAPDH trypanosomal protein (kindly provided by P.A.M. Michels; raised in rabbit; dilution 1:4000). Visualization was done using ECL+ kit (Amersham).

2.6. Respiratory experiments, inhibitions and membrane potential measurements

Respiration of intact cells was measured using Strathkelvin Oxygen System. Clark electrode was calibrated using distilled water as described by the manufacturer. Cell cultures were diluted to a final concentration of 1.5×10^7 cells/ml, 500 μl of culture was added into a closed chamber and respiration was followed for 2–4 min. Upon this period, KCN followed by SHAM were added to a final concentration of 1 mM in 2–4 min intervals; specificity was confirmed by the addition of these drugs in reverse order.

Mitochondrial membrane potential was assessed as described previously [32]. Briefly, the cells were stained using TMRE or Safranin O (both 100 nM final concentration) in media and diluted 5× in isotonic buffer for flow cytometry. For every run, 20,000 particles were analyzed. Unstained cells were used as a control to calibrate voltage of PE channel. Then, staining in the presence or absence of the un-coupler FCCP was analyzed. Data were processed using CyfLogic (v 1.2.1; CyFlo) software.

3. Results

3.1. Distinct patterns of respiratory complexes on 2D gels

Mitochondrial vesicles of the four trypanosomatids were lysed using dodecyl maltoside and separated on 2D gels using native and denaturing conditions as described previously [18]. Upon separation, the gels were stained with Coomassie brilliant blue to reveal protein patterns. This method can generally distinguish between various protein complexes depending on the conditions used. We have been able to detect complexes I, III, IV and V, based on previous studies [17,18,21,29,33], while subunits of complex II were under these conditions not identified. Despite their close relationship, different trypanosomatids showed distinct patterns of their respiratory complexes on the 2D under native and denaturing conditions (Fig. 1). A common denominator of the different flagellates is the pattern and position of complex V with various sizes under the conditions of native gels (see below). The proteins of this complex are subsequently resolved into two (Fig. 1A–C) or three (Fig. 1D) parallel lines in the second denaturing dimension.

The cleanest pattern with minimal horizontal smears was consistently obtained for *L. tarentolae*. Going from the highest molecular weight down, there are always two roughly equal columns of subunits belonging to ATP synthase (Fig. 1A; V), followed by the third column representing complex IV (Fig. 1A; IV) and, finally, the fourth one with subunits of complex III (Fig. 1A;

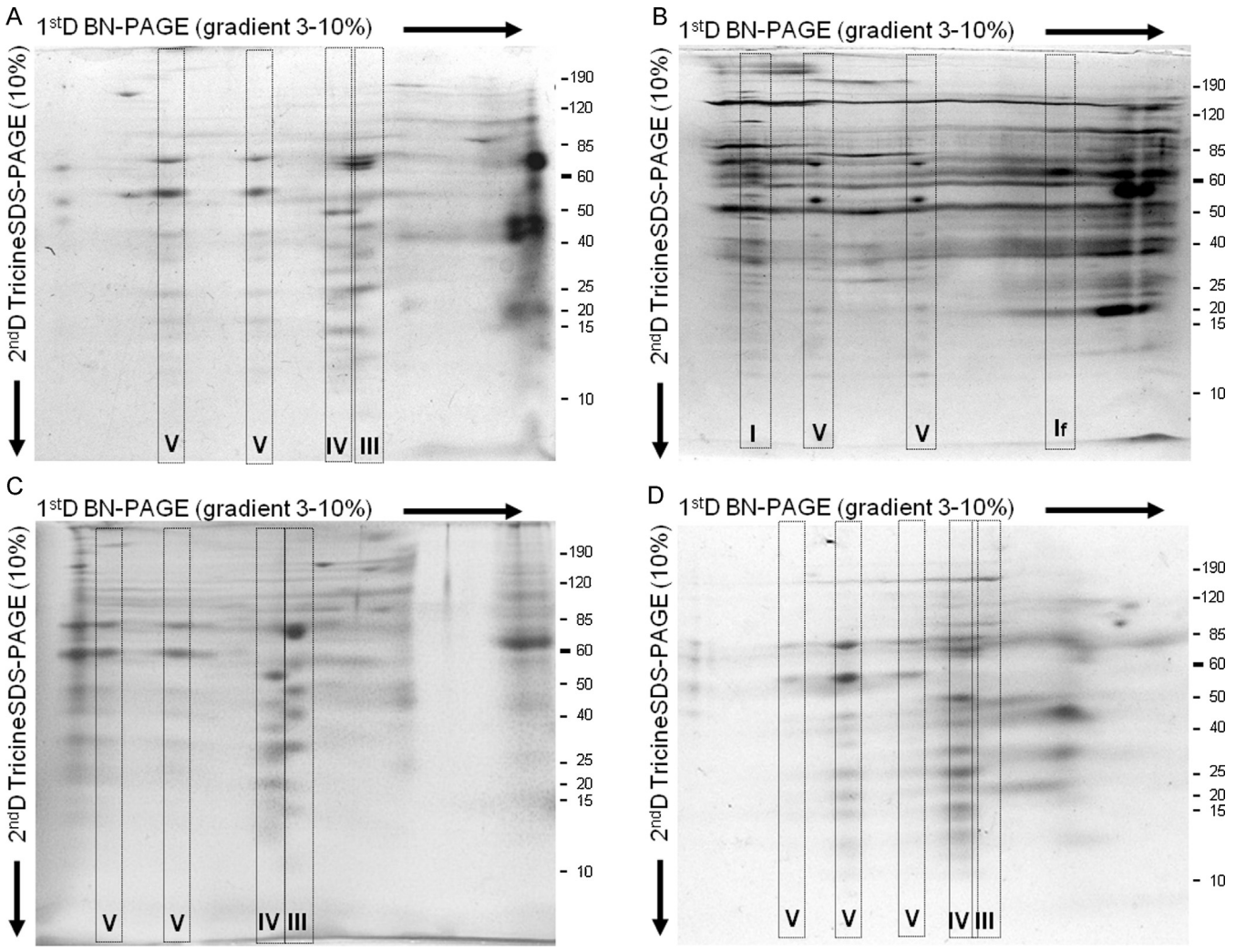

Fig. 1. Native versus denaturing 2D analysis of mitochondrial lysates. Gels are stained with Coomassie Blue. (A) *L. tarentolae*; (B) *P. serpens*; (C) *T. brucei*; (D) *C. fasciculata*.

III). *P. serpens*, which is known to lack complexes III and IV [34], has an unexpectedly complex pattern. Complex I, the functionality of which was demonstrated previously [29], constitutes a line in the highest molecular weight region of the gel. As was already shown [29], a weak column with a relatively low molecular weight corresponds to part of complex I (Fig. 1B; If), yet the same complex is undetectable in *L. tarentolae, T. brucei*, and *C. fasciculata* (Fig. 1A, C and D, respectively). *T. brucei* and *P. serpens* share much more extensive horizontal smearing pattern than the other two species. *C. fasciculata* has a little less clear pattern, in which complex V is resolved into three columns that are not equivalent in terms of the amount of the protein (Fig. 1D).Columns corresponding to complexes IV and III overlap noticeably more in *C. fasciculata* than in *L. tarentolae* and *T. brucei*.

The front as well as the lower part of all four native gels contains numerous unidentified proteins. However, the number of proteins in any given column does not seem to be sufficient to build a protein complex of corresponding molecular weight, unless it is an agglomerate of multiple repeated subunits, such as in the case of the human pyruvate dehydrogenase complex [35]. Moreover, many of those spots are of unequal intensity, another reason why they most likely do not belong to a single multi-subunit complex.

3.2. Immunodetection of OXPHOS subunits and in-gel activity staining

Upon analysis of 2D gel patterns, the mitochondrial lysates from all four trypanosomatids were separated on SDS-PAGE, blotted and probed with a set of antibodies raised against subunits of complexes I–V. Results indicated that only the subunits of complexes II and V are present in all samples, while Western blot analysis confirmed the absence of the subunits of complexes III and IV in *P. serpens* (Fig. 2). Immunodetection using antibodies against the 39 kDa subunit of the bovine complex I showed a clear ~50 kDa band in *P. serpens* and *T. brucei*, while it gave no signal in *L. tarentolae* and *C. fasciculata* (Fig. 2). Western blot analysis further underlined close phylogenetic relationships among the studied species, as antibodies raised against a protein from one trypanosomatid recognized the corresponding proteins in other trypanosomatid species.

Next, we performed an in-gel staining for all classical enzymatic activities of the RC. In a pilot experiment, we checked and compared two different separation systems – blue native (BN) and high resolution clear native (hrCN) gels (data not shown). Based on the results, we performed all activity staining using the BN set-up with the exception of complex II, the activity of which gave reproducible results only using the hrCN system.

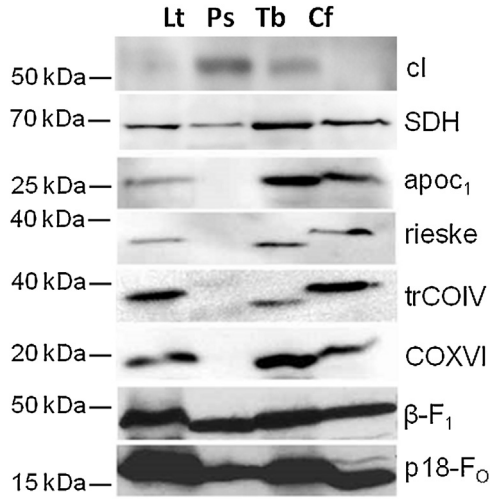

Fig. 2. Western blot analysis upon 1D SDS-PAGE. Antibodies against the following subunits have been used: complex I – 39 kDa subunit of bovine complex (>50 kDa) (cI); complex II – subunit SDH1 (66 kDa) (SDH); complex III – apocytochrome c_1 (29 kDa) (apoc$_1$) and the Rieske protein (34 kDa) (rieske); complex IV – subunits IV (36 kDa) (trCOIV) and VI (20 kDa) (COXVI); complex V – beta subunit from the F_1 moiety (47 kDa) (β-F_1) and p18 from the F_O moiety (18 kDa) (p18-F_O). Lt – *L. tarentolae*, Ps – *P. serpens*, Tb – *T. brucei*, Cf – *C. fasciculata*.

In native gels, the NADH dehydrogenase activity uses nitrotetrazolium blue (NTB) as an artificial final electron acceptor forming a violet precipitate upon reduction [36]. Using this approach, two and one high molecular bands were detected in *P. serpens* and *T. brucei*, respectively, while there was no signals in *L. tarentolae* and *C. fasciculata* (Fig. 3A; cI). In *P. serpens*, both bands have been confirmed to correspond to complex I as they showed on 2D gel a cross-reaction with the anti-39 kDa subunit of bovine complex I [29]. As for *T. brucei*, Western blot analysis upon the 2D gel repeatedly failed to show the same signal despite its unequivocal presence upon standard 1D SDS-PAGE (Fig. 2). Hence, the identity of the enzymatic complex responsible for the violet precipitate was not conclusively demonstrated for *T. brucei*. The lack of a precipitate in the mitochondrial lysates of UC strains of *L. tarentolae* and *C. fasciculata* correlates with the described absence of complex I in these organisms [17,37].

During staining of complex II, electrons from succinate travel through N-methylphenazonium sulfate to NTB, forming a violet precipitate [36]. Specific complex II bands of all four trypanosomatids migrated slightly higher than 440 kDa, in about the same region (Fig. 3A; cII). Moreover, with the exception of *P. serpens*, the lysates showed additional activity bands (Fig. 3A; cII). To evaluate their specificity, we run a native gel followed by Western blot analysis with antibodies raised against the SDH1 subunit (SDH66) of succinate dehydrogenase [30]. In all four lanes, this antibody immunodecorated the strongest activity bands as well as several minor bands (Fig. 3B; sdh), confirming the specificity of a very complex activity-staining pattern of *C. fasciculata*. Different distances

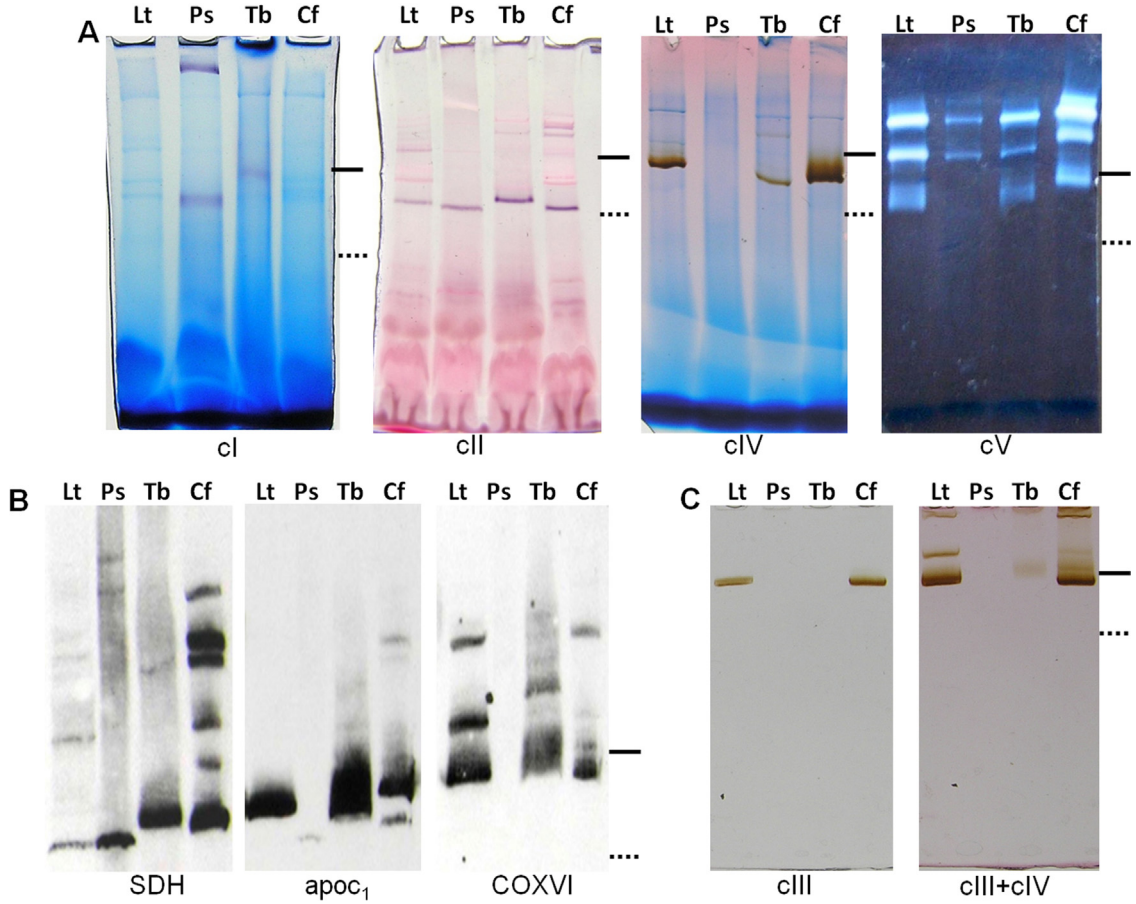

Fig. 3. Electrophoretic analysis of mitochondrial lysates. (A) In-gel staining in native gels of complexes I (cI), II (cII), IV (cIV) and V (cV). (B) Immunodetection after native electrophoresis of subunit SDH1 of complex II (SDH), apocytochrome c_1 of complex III (apoc$_1$) and subunit VI of complex IV (COXVI). All Western blots were made on the same membrane that was striped and reprobed by appropriate antibodies. (C) Comparison of the complex III and IV in-gel staining. Density of gradient native gels varied from 2–12% to 3–15%. Ferritin 440 kDa – dash line, and its dimeric form 880 kDa – solid line was used as a molecular weight marker. Lt – *L. tarentolae*; Ps – *P. serpens*; Tb – *T. brucei*; Cf – *C. fasciculata*.

Table 1
Activities of oxidative phosphorylation enzymes.

Activity	Substrate	Inhibitor	*L. tarentolae*	*P. serpens*	*T. brucei*	*C. fasciculata*
NADH dehydrogenase	Coenzyme Q_2	no	14 ± 8	30 ± 10	39 ± 18	19 ± 6
		rotenone [10 μmol/l]	ND*	65%	88%	ND*
		DPI [100 μmol/l]	ND*	59%	20%	ND*
	$K_3[Fe(CN)_6]$	no	157 ± 64	60 ± 17	166 ± 56	210 ± 44
		rotenone [10 μmol/l]	ND*	89%	96%	ND*
		DPI [100 μmol/l]	ND*	51%	25%	ND*
Succinate dehydrogenase	Coenzyme Q_2	no	72 ± 15	18 ± 12	27 ± 5	50 ± 8
		malonate [1 mmol/l]	0%	0%	2%	0%
Cytochrome c reductase	Cytochrome c	no	403 ± 184	16 ± 9	346 ± 129	223 ± 28
		antimycin [0,3 μg/ml]	0,10%	ND	0%	ND
Cytochrome c oxidase	O_2	no	5,1 ± 2,7	0,2 ± 0,1	2 ± 1,4	4,7 ± 2,6
		KCN [100 μmol/l]	0%	ND	0%	ND
ATPase	ATP	no	247 ± 64	77 ± 9	182 ± 53	143 ± 57
		oligomycin [10 μg/mg]	43%	70%	53%	55%
		azide [1 mmol/l]	55%	74%	47%	43%
G3PDH	G3P	no	13 ± 4	88 ± 36	29 ± 13	11 ± 2
		diazoxid [1 mmol/l]	67%	89%	59%	ND

Values in rows with "no" inhibitors are in U/mg for NADHdehydrogenase, succinate dehydrogenase and ATPase and in mU/mg for cytochrome *c* reductase, cytochrome *c* oxidase and G3PDH. Values in rows with inhibitors represent average % of uninhibited activity in the presence of an appropriate inhibitor. ND* = values were measured, but despite several repeated attempts, obtained data were not reproducible. The unit (U) of appropriate activity is defined as an amount of enzyme required for conversion of: (i) 1 nmol of NADH/min for NADH dehydrogenase; (ii) 1 nmol of 2,6-dichlorophenolindophenol/min for succinate dehydrogenase; (iii) 1 μmol of cytochrome *c* for both cytochrome *c* reductase and cytochrome *c* oxidase; (iv) 1 nmol of ATP (releasing of 1 nmol of free phosphate)/min for ATPase; (v) 1 μmol of 2,6-dichlorophenolindophenol/min for G3PDH.

of the additional bands from the main one suggest that the higher bands are not mere homo-agglomerates of complex II.

We were unable to reproduce the published methodology for activity staining of complex III [28,38]. By this method, signals in a position that correlated with that of complex IV were consistently obtained (Fig. 3C). Different position of both complexes was confirmed by 2D gel and Western blot analyses (Figs. 1C and 3B; $apoc_1$ and COXVI), and serial double in-gel staining. In this approach, we stained the gel with the described complex III protocol, followed by the specific complex IV in-gel staining (Fig. 3C). Total overlap of the two in-gel staining signals unambiguously showed that the expected complex III signal is indeed associated with complex IV.

Detection of the complex IV activity is based on an oxidoreductive reaction between an oxidized cytochrome *c* and diamino benzidine, resulting in the formation of a brown-red precipitate. The reduced cytochrome *c* is then re-oxidized by complex IV [39]. As expected, there was no staining in the *P. serpens* mitochondrial lysate (Fig. 3A; cIV). The signal in the *T. brucei* lysate was weaker than that of *L. tarentolae* and *C. fasciculata* (Fig. 3B). Besides the strongest lower bands in all three active lines, one can distinguish some very weak bands in the upper part of the gel, similar to agglomerates seen following the SDH activity staining.

To confirm the specificity of complex III/IV staining, we performed Western blot analysis in the same way as described for complex II. Membranes were stripped and repeatedly reprobed with the anti-$apoc_1$ and COXVI antibodies, respectively. As expected, we did not detect any signal in the *P. serpens* lane confirming the lack of complexes III and IV in this flagellate [34]. Other trypanosomatids showed a strong uniform signal when probed with anti-apoC, while the coxVI pattern contained also some weak high molecular weight bands (Fig. 3B). This experiment confirmed different positions of complexes III and IV.

Complex V activity was also successfully detected in the native gel, using a staining method based on the formation of a Pb-containing precipitate. The precipitation is a result of low pH as a consequence of a free phosphate group release during ATP hydrolysis [26]. Upon staining (Fig. 3A; cV), three bands corresponding to oligomers of the F_1 sub-complex (the lower band) and the F_1F_O sub-complex (the middle and upper bands) [33] appeared. We observed that the intensities of the individual bands differed between isolations; hence, they most likely reflect slightly different conditions of a given isolations rather than a physiological feature. Identity of the bands was evaluated by Western blot analysis of native complexes using antibodies against various subunits of the ATP synthase. The resulting signals almost exactly followed the pattern of activity staining (data not shown).

3.3. Quantitative determination of OXPHOS activities

In trypanosomatids, the NADH dehydrogenase activity represents a rather complex issue due to the possible presence of two distinct enzymes, namely a multi-subunit complex I [EC 1.6.5.3] and a rotenone-insensitive alternative NADH dehydrogenase [EC 1.6.5.9], which use the same substrates and acceptors. Both utilize NADH and transfer electrons through a flavine co-factor to ubiquinol. While complex I has been reported as missing in the cultured forms of *L. tarentolae* and *C. fasciculata* UC strains [40], the NDH2 gene was found in the genomes of *T. brucei* and *L. tarentolae* (Tb927.10.9440 and LtaP36.5520 entries at tritrypdb.org).

For measurement of the total NADH dehydrogenase activity, we used ferricyanide, an electron acceptor with low redox potential capable of accepting electrons with lower energy as compared to ubiquinone. In this set up, *C. fasciculata* was shown to possess the highest activity (210 ± 44 U/mg) among studied flagellates. Next, *T. brucei* exhibited an activity of 166 ± 56 U/mg followed by *L. tarentolae* (157 ± 64 U/mg) and *P. serpens* (60 ± 17 U/mg). A completely different pattern was obtained when ubiquinon-2 (Q_2) was used as the electron acceptor. Activities of *C. fasciculata* and *L. tarentolae* dropped below 10% of their original activity (19 ± 6 U/mg and 14 ± 8 U/mg, respectively), while those of *T. brucei* and *P. serpens* reached about one quarter (39 ± 18 U/mg) and one half (30 ± 10 U/mg) of their ferricyanide activities, respectively. Different distribution of activities obtained with Q_2 and ferricyanide clearly demonstrates the presence of other NADH-dependent oxidoreductase(s) not involved in the RC.

Measurement of the NADH dehydrogenase activity in the presence of inhibitors further corroborated these observations (Table 1). Rotenone is a specific inhibitor of the eukaryotic complex I, while diphenyl iodonium (DPI) is a general inhibitor of flavine-containing enzymes shown previously to inhibit NDH2 in *P. serpens* [29]. Our current data confirmed that observation, the contribution of complex I and NDH2 being about equal. Furthermore, the activity was mostly susceptible to DPI in the *T. brucei* mitochondrial lysates, a phenomenon described previously [41]. Contrary to these

data, however, we did not obtain reproducible results with either inhibitor in experiments with the mitochondrial lysates from *L. tarentolae* and *C. fasciculata* (Table 1).

The activity of complex II can be spectrophotometrically followed as a change in the absorbance of 2,6-dichlorophenolindophenol (DCIP), with electrons passed from succinate to DCIP via Q_2 [42]. This activity shows a pattern complementary to the complex I/NDH2 activities. The activities of *L. tarentolae* and *C. fasciculata* are 72 ± 15 U/mg and 50 ± 8 U/mg of protein, respectively, being much higher than those of *T. brucei* (27 ± 5 U/mg) and *P. serpens* (18 ± 12 U/mg). Specificity of the reaction was confirmed by the addition of 1 mM malonate, a competitive inhibitor of complex II (Table 1).

The complex III activity measurement is based on a direct spectrophotometric monitoring of the cytochrome *c* reduction at 550 nm. Same as in the case of complex II, *L. tarentolae* showed the highest activity (403 ± 184 mU/mg), followed by *T. brucei* and *C. fasciculata*, with activities reaching 346 ± 129 mU/mg and 223 ± 28 mU/mg, respectively. *P. serpens*, lacking this complex, exhibited a negligible activity of 16 ± 9 mU/mg. Specificity of the reaction was monitored by its inhibition using 0.3 μg/ml of antimycin A (Table 1).

The same substrate is used for spectrophotometric measurement of complex IV with monitoring oxidation of cytochrome *c*. *L. tarentolae* exhibited the highest activity (5.1 ± 2.7 mU/mg), followed by *C. fasciculata* (4.7 ± 2.6 mU/mg) and *T. brucei* (2.0 ± 1.4 mU/mg). *P. serpens*, which lacks mitochondrial [34] as well as nuclear-encoded subunits [43], exhibited only a background activity of 0.2 ± 0.1 mU/mg. Addition of 100 μM potassium cyanide completely blocked the reaction (Table 1). Since the activities of both complexes III and IV were monitored via the reduction/oxidation of cytochrome *c*, they do not provide any information about the TAO activity.

The activity of complex V was measured by its ability to hydrolyse ATP [14]. The reaction is followed using molybdenum blue that is proportional to a free phosphate generated during the hydrolysis. In this experiment, *L. tarentolae* again showed notably the highest ATPase activity with a value 247 ± 64 U/mg. *T. brucei* (182 ± 53 U/mg) followed by *C. fasciculata* (143 ± 57 U/mg) showed middle range values, while the activity of *P. serpens* (77 ± 9 U/mg) was two to three times lower than that of the other trypanosomatids. Upon this measurement, the sensitivity to complex V inhibitors, namely oligomycin and sodium azide, was tested (Table 1). *P. serpens* stands aside of the remaining three parasites in this respect. While the sensitivity of *L. tarentolae*, *T. brucei* and *C. fasciculata* to both compounds was about 50%, the ATPase activity of *P. serpens* decreased only by about 30% in the presence of these inhibitors.

Finally, we measured the activity of mtG3PDH, an enzyme that provides electrons to the OXPHOS systems as a part of the glycerol-3-phosphate shuttle, making use of a recently described method [24]. The activity was uniformly detected in all four trypanosomatids with *P. serpens* again standing out of the line. Its mtG3PDH activity was more than twice as high (71 mU/mg) as in *T. brucei* (31 mU/mg). *L. tarentolae* (15 mU/mg) and *C. fasciculata* (10 mU/mg) showed a rather minor conversion of glycerol-3-phosphate to dihydroxyacetone phosphate. Similarly to situation with the ATPase inhibitors, the sensitivity of *P. serpens* to diazoxide, an inhibitor of mtG3PDH, was much lower than in the others tested strains (Table 1).

3.4. Respiration and membrane potential

Oxygen consumption was measured using living trypanosomatids (Fig. 4). *L. tarentolae* shows by far the highest oxygen consumption reaching 6.7 ± 1.9 nmol^{-1} min^{-1} 10^{-6} cells, followed by *C. fasciculata* (4.9 ± 0.8 nmol^{-1} min^{-1} 10^{-6} cells), *T. brucei* (3.6 ± 1.5 nmol^{-1} min^{-1} 10^{-6} cells) and *P. serpens* (2.9 ± 1.3 nmol^{-1} min^{-1} 10^{-6} cells). This relatively rough measurement was followed by the analysis of sensitivity to inhibitors. Cyanide (KCN) was used to inhibit the classical electron pathway from ubiquinol through cytochrome *c* to oxygen, while salicylhydroxamic acid (SHAM) is known to inhibit an alternative pathway directing electrons from ubiquinol to TAO. This analysis showed that *L. tarentolae* and *C. fasciculata* are entirely dependent on the cytochrome pathway; in both cases, 1 mM KCN fully inhibited oxygen consumption while 1 mM SHAM had no effect on respiration. Contrary to this, *P. serpens* showed no change in oxygen consumption upon KCN and full inhibition upon the addition of SHAM. *T. brucei* showed a mixed effect: KCN inhibited 66 ± 11% of oxygen consumption, while the inhibition incurred by SHAM was 23 ± 11% of the respiration.

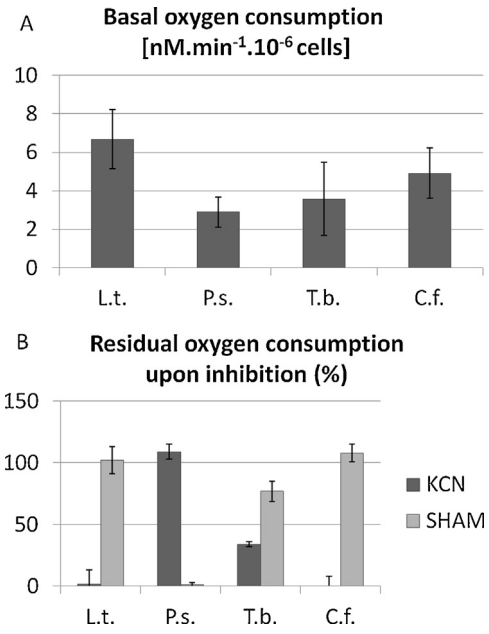

Fig. 4. Respiration measurement. (A) Consumption of oxygen in nmol/min for 10^6 cells. (B) Inhibition (in %) of the respiratory pathways by 1 mM KCN and 1 mM SHAM. Respiration with no inhibitors was taken as 100% for each strain. KCN = respiration in the presence of 1 mmol/l KCN; SHAM = respiration in the presence of 1 mmol/l salicylhydroxamix acid. Lt – *L. tarentolae*, Ps – *P. serpens*, Tb – *T. brucei*, Cf – *C. fasciculata*.

Finally, we performed a comparative analysis of mitochondrial membrane potentials. Initially, autofluorescence was recorded followed by the measurements of TMRE-stained or TMRE-stained FCCP-treated parasites (Fig. 5; left panel). *T. brucei* and *L. tarentolae* showed a pattern comparable with *L. tarentolae*, which is slightly more sensitive to the uncoupler. On the contrary, *P. serpens* showed only a miniscule difference upon the FCCP treatment. We were unable to stain the mitochondrion of *C. fasciculata* under the conditions suitable for the other flagellates. Since the mitochondrial membrane potential of *P. serpens* was previously shown to reach 150 mV [44], we stained the cells with Safranin O to test whether this dye would increase the signal. As shown in Fig. 5B (right panel), the signal is even weaker than with TMRE (Fig. 5B; left panel). We attribute this to the omitted permeabilization step, as the increase in mitochondrial membrane staining occurred after the addition of digitonin (Fig. 4 in [44]). Interestingly, the Safranin O-staining gave better results in *L. tarentolae* and *C fasciculata* (Fig. 5A and D; right panel). Since Safranin O is less polar than TMRE, we believe that the difference in staining is due to their different permeability.

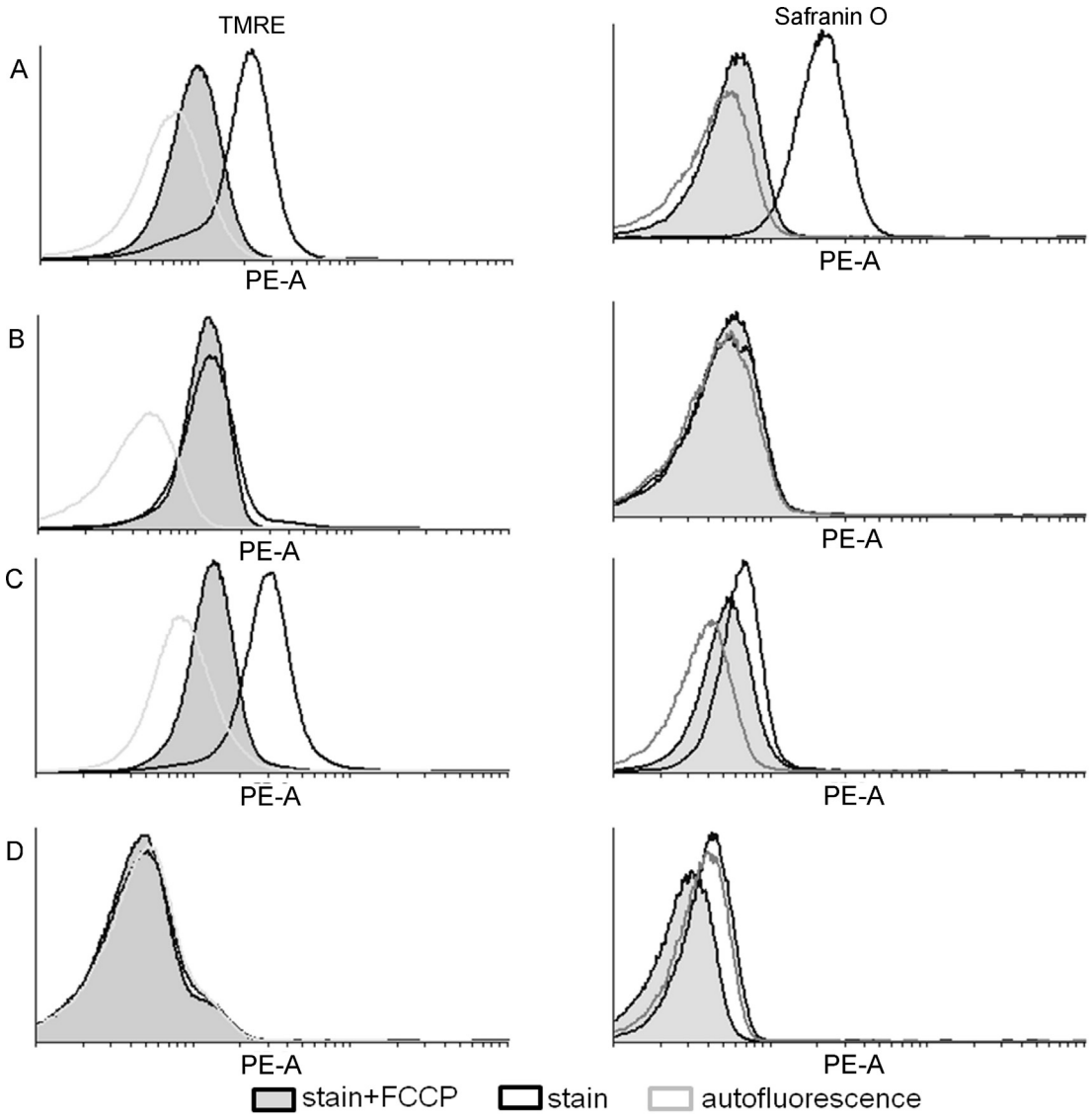

Fig. 5. Measurement of membrane potential using flow-cytometry.
Cells were stained by TMRE (left panel) or Safranin O (right panel) and treatment with the uncoupler FCCP was used as a control. (A) *L. tarentolae*; (B) *P. serpens*; (C) *T. brucei*; (D) *C. fasciculata*.

4. Discussion

This study deals for the first time with a parallel side-by-side comparison of OXPHOS in the best studied laboratory representatives of four trypanosomatid genera *L. tarentolae, C. fasciculata* (both UC strains), *P. serpens* (9T strain) and *T. brucei* (29–13 strain). These flagellates have distinct evolutionary and laboratory histories and evolved different life strategies that are reflected in their metabolic adaptations. This side-by-side comparison, which applies multiple approaches for characterizing enzymes of OXPHOS, overcomes a problem of previous characterizations that were each done only on a single species, using varying techniques and methodology in different laboratories. It also allows us to evaluate the usefulness of various methodologies/approaches for characterization of not only these protozoan's but the OXPHOS in general. Although some of the obtained results may not be applicable to even closely related species, they document a very high variability of OXPHOS and have a potential to be a useful tool for further studies of respiratory chain and ATP synthase within and outside the family Trypanosomatidae.

Complex I is certainly the most enigmatic respiratory enzyme of trypanosomatids. While complexes II to V have been clearly documented in kinetoplastids, the presence of a functional complex I remained questionable for a long time. One of the factors that complicated its study is the existence of an alternative NADH dehydrogenase (NDH2), which is capable of transferring electrons from NADH to ubiquinone, essentially performing the same reaction as the *bone fide* complex I [45]. In this study, the NADH:Q_2 oxidoreductase activity has been detected with certainty only in *P. serpens* and *T. brucei*. For the remaining trypanosomatids, the recorded NADH:Q_2 activity reached only about 10% of the total NADH dehydrogenase activity detected with ferricyanide, an electron acceptor with low redox potential. This suggests that the cultivated *L. tarentolae* and *C. fasciculata* have only marginal, if any, capacity to transfer electrons from NADH to Q. Moreover, their sensitivity to rotenone and/or DPI turned out to be inconclusive. It should be noted that DPI is a general inhibitor of flavin-containing enzymes that was shown to target NDH2 and not complex I at 100 μM in *P. serpens* [41]. Thus, we interpret the miniscule NADH:Q_2 activity in these two species as an unspecific dehydrogenase activity, which corresponds with the reported lack of complex I [17,37]. Alternatively, the residual NADH:Q_2 activity might be attributed to NDH2 that is present in the genome of *L. tarentolae*. The relatively low

activity would be in agreement with an observation from *T. brucei* where in the NDH2-depleted procyclics the specific NADH:Q_2 activity did not drop, while the NADH-dependent respiration decreased significantly [32]. At the moment, there are no data on the presence/absence of NDH2 in *C. fasciculata*, hence we believe the above description applies also for this flagellate. Nevertheless, given that only about 50 and 30% of the NADH:Q_2 activity can be inhibited by rotenone in *P. serpens* and *T. brucei*, respectively [29,41], the identity of the enzyme responsible for the remaining NADH:Q2 activity remains unsolved. Taken together, we conclude that the enzyme(s) responsible for the general NADH dehydrogenase activity contains a flavin cofactor.

In-gel staining of NADH:NTB activity is another assay, the specificity of which was questioned, as we were unable to directly confirm its association with complex I in the mitochondrial lysate of *T. brucei*. While the anti-39 kDa bovine complex I subunit antibody produced a signal under standard SDS-PAGE conditions, it failed to do so in 2D BN:SDS-PAGE, preventing us from (dis)associating it with the NADH:NTB signal. Another aspect questioning the specificity of this method is that the NADH:NTB assay can be used for in-gel detection of dihydrolipoamide dehydrogenase (DLDH) [46]. This was confirmed by Surve et al. [47], who in the *T. brucei* mitochondrial lysate detected DLDH in the NTB-stained complex migrating at approximately 480 kDa [47]. However, in the same parasite, Acestor et al. [38] visualized the NADH:NTB activity band co-migrating with complex I-derived Western blot signal near the 1048 kDa marker. It is likely that the reported differences are caused by the use of different detergents. We showed that the NADH:NTB activity band migrates between 720 and 1048 kDa, which is a region containing putative complex I subunits in both the bloodstream and procyclic stages of *T. brucei* [47]. Indeed, experiments with different combinations of detergents and native gel conditions resulted in dramatic differences in in-gel staining patterns (A. Horvath, unpubl. data). All in all, these observations indirectly support the conclusion that we have indeed detected complex I activity in *T. brucei*.

The comparative analysis of complex II showed that all four trypanosomatids express at least the flavin-containing SDH1 subunit, which is assembled in a complex comparable in size with the 9-subunit complexes of *T. brucei* and *T. cruzi* [38,48]. The co-migration of complexes II, III, IV and the F_1 moiety of complex V is likely responsible for our inability to detect complex II in the Coomassie-stained 2D native:SDS-PAGE gels, although its low concentration may be another reason for this failure. Since artificial multimerization of proteins and their complexes is a typical feature of native PAGE gels (A. Horvath, unpubl. data), it is possible that at least part of the high molecular weight bands recognized by the anti-SDH1 antibody and/or the specific in-gel staining are artifacts caused by the native PAGE features. The spectrophotometrically measured complex II activity is much higher in *L. tarentolae* and *C. fasciculata* than in *P. serpens* and *T. brucei* and is inversely proportional to the NADH:Q_2 activity.

Complexes III and IV are the best studied enzymes of the trypanosomatid respiratory chain. Their composition in *T. brucei, C. fasciculata* and *L. tarentolae* was established by numerous biochemical and molecular approaches including extensive mass spectrometry [18,21,38,49–53]. The complexes were proven absent from *P. serpens* [31,34,54], as further supported by our data. If present, complex IV is invariably larger than complex III, a feature setting these flagellates apart from other eukaryotes [55,56]. General 2D patterns of both complexes remain constant and small but notable differences in their relative migration probably reflect differences in the presence/absence of some subunits not connected with their activity. Indeed, the *C. fasciculata* and *L. tarentolae* complexes IV have 10 [53] and 11 [21] subunits, respectively, while in *T. brucei*, even more subunits have been characterized [31,50,51]. The in-gel staining of complex III previously described elsewhere [38,57] was non-specific in our hands. At the moment, we can explain the apparent staining of complex IV using complex III methodology only as a consequence of poor reproducibility of this method.

Active complex V is present in all four species with the highest spectrophotometric ATPase activity in *L. tarentolae* and the lowest one in *P. serpens*. This was further confirmed by in-gel staining. The lower sensitivity of *P. serpens* to specific inhibitors such as oligomycin and sodium azide might be a result of unique features of its complex V, or more likely it could reflect the relatively low contribution of complex V to overall mitochondrial ATPase activities. The membrane potential in *P. serpens* is sensitive to complex I inhibitor rotenone and insensitive to complex V inhibitor oligomycin [44]. This fact indicates that in this species complex V plays the canonical role of ATP synthase in the same way as in the other flagellates.

The FAD-G3PDH activity presumably reflecting the metabolic activity of glycosomes is in inverse proportion to the activities of complexes III, IV and V, with *P. serpens* being an extreme example. While its classical OXPHOS enzymes have rather low activity and complexes III and IV are missing altogether, *P. serpens* possesses the highest FAD-G3PDH activity, indicating that its substrate level phosphorylation plays much more important function than in the other studied species. The observed low sensitivity of FAD-G3PDH to diazoxid, an inhibitor of mitochondrial FAD-G3PDH, could be either a result of different tertiary structure, or there is another diazoxid-insensitive FAD-G3PDH. Such secondary enzyme was recently described in *T. brucei* [24], however, its (in)sensitivity to diazoxide has not been examined.

Assaying the mitochondrial membrane potential pointed to the use of different dyes as a putative source of artifacts. While TMRE staining has been extensively used in *T. brucei* [18,24,32,41,50,58], it is apparently not suitable for *C. fasciculata*. Safranin O, a more hydrophobic compound used earlier in *P. serpens* [44], showed some staining in *C. fasciculata*. Previously, the mitochondrial membrane potential was in *C. fasciculata* successfully measured by methyltriphenylphosphonium cation, a rather lipophilic compound [59]. Meanwhile, Safranin O stained *T. brucei* to a lesser extent than TMRE. We believe that different staining is a consequence of a charged surface of *C. fasciculata* [60] and different hydrophobicity of these drugs. Thus, it is likely that the discrepancy in staining is due to the relatively high hydrophilicity of TMRE that trapped the molecule on the surface of the cell.

TAO represents an alternative ubiquinol-oxidating pathway competing for ubiquinol with complex III. Its activity was measured only indirectly via sensitivity of oxygen consumption to SHAM. Our data confirmed the full dependence of *P. serpens* on TAO, its absence in the respiratory chain of *L. tarentolae* [61] and *C. fasciculata*, and the intermediate position of *T. brucei*.

We did not find any evidence for cytochrome-*o* dependent respiration in any of four tested species. Respiration in *L. tarentolae, C. fasciculata* and *P. serpens* is completely inhibited by KCN or SHAM what indicates presence only single electron pathway to oxygen. In *T. brucei* we detected only two distinct respiration pathways when oxygen consumption was 100% blocked by simultaneous adding KCN and SHAM (data not shown). Discrepancy of our results and incidence of cytochrome-*o* in *L. tarentolae* reported previously [62] could be explained as a natural variance between strains, different cultivation condition that led to repression/induction of some metabolic pathways or as a loss of the metabolic pathways due to long laboratory cultivation of used *L. tarentolae*.

While all four studied trypanosomatids appear to have a sound capacity for the use of their mitochondria for ATP production even in the presence of glucose, the major differences among them lie in differentially present enzymes and pathways. While *P. serpens* lacks the whole cyanide-sensitive branch of the respiratory chain,

laboratory strains of *L. tarentolae* and *C. fasciculata* do not have TAO and likely lost complex I during laboratory cultivation. Apart from the losses, activation of FAD-G3PDH when the classical OXPHOS is down-regulated, a situation exemplified by *P. serpens*, represents another species-specific metabolic adaptation. At the moment, we have no explanation for variations in the activities of classical OXPHOS enzymes, although the observed maximum capacities of the enzymes are likely not reached *in vivo*. However, a common feature of all studied species is that the missing or low activity of one pathway is compensated by an increase of another one(s).

Acknowledgements

We would like to thank Vladislava Benkovičová-Ďurišová (Comenius University, Bratislava) and Tomáš Skalický (Institute of Parasitology, České Budějovice) for help with some experiments. We also thank Paul A.M. Michels (Universidad de los Andes, Mérida/University of Edinburgh, Edinburgh), André Schneider (University of Bern, Bern) and Alena Zíková (Institute of Parasitology, České Budějovice) for sharing antibodies and James Allen for valuable discussion on cytochrome o. This work was supported by the Slovak Research and Development Agency under the contract No. APVV-0286-12; the Scientific Grant Agency of the Slovak Ministry of Education and the Academy of Sciences 1/0664/13; ITMS 26240120003 and ITMS 26240120027, the Research & Development Operational Programme funded by the ERDF; National Scholarship Programme of the Slovak Republic for the Support of Mobility to Z.V.; the Czech Grant Agency P305/12/2261, the Bioglobe grant CZ.1.07/2.3.00/30.0032, the AMVIS LH12104 grant and the Praemium Academiae award to J.L., who is also a Fellow of the Canadian Institute for Advanced Research. We acknowledge the use of research infrastructure that has received funding from the European Union Seventh Framework Programme (FP7/2007-2013) under grant agreement no. 316304.

References

[1] Maslov DA, Votýpka J, Yurchenko V, Lukeš J. Diversity and phylogeny of insect trypanosomatids: all that is hidden shall be revealed. Trends Parasitol 2013;29:43–52.
[2] Votýpka J, Suková E, Kraeva N, Ishemgulova A, Duží I, Lukeš J, et al. Diversity of Trypanosomatids (Kinetoplastea: Trypanosomatidae) Parasitizing Fleas (Insecta: Siphonaptera) and description of a new genus *Blechomonas* gen. n. Protist 2013;164:763–81.
[3] Flegontov P, Votýpka J, Skalický T, Logacheva MD, Penin AA, Tanifuji G, et al. Paratrypanosoma is a novel early-branching trypanosomatid. Curr Biol 2013;23:1787–93.
[4] Vickerman K. Developmental cycles and biology of pathogenic trypanosomes. Br Med Bull 1985;41:105–14.
[5] Wallbanks KR, Maazoun R, Canning EU, Rioux JA. The identity of *Leishmania tarentolae* Wenyon 1921. Parasitology 1985;90:67–78.
[6] Bañuls A-L, Hide M, Prugnolle F. Leishmania and the leishmaniases: a parasite genetic update and advances in taxonomy, epidemiology and pathogenicity in humans. Adv Parasitol 2007;64:1–109.
[7] Dollet M. Plant diseases caused by flagellate protozoa (Phytomonas). Annu Rev Phytopathol 1984;22:115–32.
[8] Scolaro EJ, Ames RP, Brittingham A. Growth-phase dependent substrate adhesion in *Crithidia fasciculata*. J Eukayotic Microbiol 2005;52:17–22.
[9] Zickermann V, Kerscher S, Zwicker K, Tocilescu MA, Radermacher M, Brandt U. Architecture of complex I and its implications for electron transfer and proton pumping. Biochim Biophys Acta 2009;1787:574–83.
[10] Rutter J, Winge DR, Schiffman JD. Succinate dehydrogenase-assembly, regulation and role in human disease. Mitochondrion 2010;10:393–401.
[11] Zara V, Conte L, Trumpower BL. Biogenesis of the yeast cytochrome bc1 complex. Biochim Biophys Acta 2009;1793:89–96.
[12] Cramer WA, Hasan SS, Yamashita E. The Q cycle of cytochrome bc complexes: a structure perspective. Biochim Biophys Acta 2011;1807:788–802.
[13] Fontanesi F, Soto IC, Barrientos A. Cytochrome c oxidase biogenesis: new levels of regulation. IUBMB Life 2008;60:557–68.
[14] Weber J, Senior AE. ATP synthesis driven by proton transport in F1Fo-ATP synthase. FEBS Lett 2003;545:61–70.
[15] Vondrušková E, van den Burg J, Zíková A, Ernst NL, Stuart K, Benne R, et al. RNA interference analyses suggest a transcript-specific regulatory role for mitochondrial RNA-binding proteins MRP1 and MRP2 in RNA editing and other RNA processing in *Trypanosoma brucei*. J Biol Chem 2005;280:2429–38.
[16] Lukeš J, Regmi S, Breitling R, Mureev S, Kushnir S, Pyatkov K, et al. Translational initiation in *Leishmania tarentolae* and *Phytomonas serpens* Kinetoplastida) is strongly influenced by pre-ATG triplet and its 5 sequence context. Mol Biochem Parasitol 2006;148:125–32.
[17] Speijer D, Breek CKD, Muijsers AO, Hartog AF, Berden JA, Albracht SPJ, et al. Characterization of the respiratory chain from cultured *Crithidia fasciculata*. Mol Biochem Parasitol 1997;85:171–86.
[18] Horváth A, Horáková E, Dunajčíková P, Verner Z, Pravdová E, Šlapetová I, et al. Downregulation of the nuclear-encoded subunits of the complexes III and IV disrupts their respective complexes but not complex I in procyclic *Trypanosoma brucei*. Mol Microbiol 2005;58:116–30.
[19] González-Halphen D, Maslov DA. NADH-ubiquinone oxidoreductase activity in the kinetoplasts of the plant trypanosomati *Phytomonas serpens*. Parasitol Res 2004;92:341–6.
[20] Birch-Machin MA, Turnbull DM. Assaying mitochondrial respiratory complex activity in mitochondria isolated from human cells and tissues. Methods Cell Biol 2001;65:97–117.
[21] Horváth A, Berry EA, Huang L, Maslov DA. *Leishmania tarentolae*: A parallel isolation of cytochrome bc 1 and cytochrome c oxidase. Exp Parasitol 2000;96:160–67.
[22] Trumpower BL, Edwards CA. Purification of a reconstitutively active iron-sulfur protein (oxidation factor) from succinate·cytochrome c reductase complex of bovine heart mitochondria. J Biol Chem 1979;254:8697–706.
[23] Schnaufer A, Clark-Walker DG, Steinberg AG, Stuart K. The F1-ATP synthase complex in bloodstream stage trypanosomes has an unusual and essential function. EMBO J 2005;24:4029–40.
[24] Škodová I, Verner Z, Bringaud F, Fabian P, Lukeš J, Horváth A. Characterization of two mitochondrial flavin adenine dinucleotide-dependent glycerol-3-phosphate dehydrogenases in *Trypanosoma brucei*. Eukaryot Cell 2013;12:1664–73.
[25] Schägger H. Blue native electrophoresis. In: Hunte C, Von Jagow G, Schagger H, editors. Membrane protein purification and crystallization. second ed. Academic Press; 2003. p. 105–30.
[26] Wittig I, Carrozzo R, Santorelli FM, Schägger H. Functional assays in high-resolution clear native gels to quantify mitochondrial complexes in human biopsies and cell lines. Electrophoresis 2007;28:3811–20.
[27] Zerbetto E, Vergani L, Dabbeni-Sala F. Quantification of muscle mitochondrial oxidative phosphorylation enzymes via histochemical staining of blue native polyacrylamide gels. Electrophoresis 1997;18:2059–64.
[28] Wittig I, Karas M, Schägger H. High resolution clear native electrophoresis for in-gel functional assays and fluorescence studies of membrane protein complexes. Mol Cell Proteomics 2007;6:1215–25.
[29] Čermáková P, Verner Z, Man P, Lukeš J, Horváth A. Characterization of the NADH:ubiquinone oxidoreductase (complex I) in the trypanosomatid *Phytomonas serpens* (Kinetoplastida). FEBS J 2007;274:3150–8.
[30] Kořený L, Sobotka R, Kovářová J, Gnipová A, Flegontov P, Horváth A, et al. Aerobic kinetoplastid flagellate Phytomonas does not require heme for viability. Proc Natl Acad Sci USA 2012;109:3808–13.
[31] Maslov DA, Zíková A, Kyselová I, Lukeš J. A putative novel nuclear-encoded subunit of the cytochrome c oxidase complex in trypanosomatids. Mol Biochem Parasitol 2002;125:113–25.
[32] Verner Z, Škodová I, Poláková S, Ďurišová-Benkovičová V, Horváth A, Lukeš J. Alternative NADH dehydrogenase (NDH2): intermembrane-space-facing counterpart of mitochondrial complex I in the procyclic *Trypanosoma brucei*. Parasitology 2013;140:328–37.
[33] Hashimi H, Benkovičová V, Čermáková P, Lai D-H, Horváth A, Lukeš J. The assembly of F(1)F(O)-ATP synthase is disrupted upon interference of RNA editing in *Trypanosoma brucei*. Int J Parasitol 2010;40:45–54.
[34] Nawathean P, Maslov DA. The absence of genes for cytochrome c oxidase and reductase subunits in maxicircle kinetoplast DNA of the respiration-deficient plant trypanosomatid *Phytomonas serpens*. Curr Genet 2000;38:95–103.
[35] Vijayakrishnan S, Callow P, Nutley MA, McGow DP, Gilbert D, Kropholler P, et al. Variation in the organization and subunit composition of the mammalian pyruvate dehydrogenase complex E2/E3BP core assembly. Biochem J 2011;437:565–74.
[36] Ponti V, Dianzani MU, Cheeseman K, Slater TF. Studies on the reduction of nitroblue tetrazolium chloride mediated through the action of NADH and phenazine methosulphate. Chem Biol Interact 1978;23:281–91.
[37] Sloof P, Arts GJ, van den Burg J, van der Spek H, Benne R. RNA editing in mitochondria of cultured trypanosomatids: translatable mRNAs for NADH-dehydrogenase subunits are missing. J Bioenerg Biomembr 1994;26:193–203.
[38] Acestor N, Zíková A, Dalley RA, Anupama A, Panigrahi AK, Stuart KD. *Trypanosoma brucei* mitochondrial respiratome: composition and organization in procyclic form. Mol Cell Proteomics 2011;10:M110.006908.
[39] Roels F. Cytochrome c and cytochrome oxidase in diaminobenzidine staining of mitochondria. J Histochem Cytochem 1974;22:442–4.
[40] Thiemann OH, Maslov DA, Simpson L. Disruption of RNA editing in *Leishmania tarentolae* by the loss of minicircle-encoded guide RNA genes. EMBO J 1994;13:5689–700.
[41] Verner Z, Čermáková P, Škodová I, Kriegová E, Horváth A, Lukeš J. Complex I (NADH:ubiquinone oxidoreductase) is active in but non-essential for procyclic *Trypanosoma brucei*. Mol Biochem Parasitol 2011;175:196–200.
[42] Hederstedt L, Rutberg L. Succinate dehydrogenase—a comparative review. Microbiol Rev 1981;45:542–55.

[43] Porcel BM, Denoeud F, Opperdoes F, Noel B, Madoui M-A, Hammarton T-C, et al. The streamlined genome of phytomonas spp. relative to human pathogenic kinetoplastids reveals a parasite tailored for plants. PLoS Genet 2014;10(2):e1004007, http://dx.doi.org/10.1371/journal.pgen.1004007.
[44] Moysés DN, Barrabin H. Rotenone-sensitive mitochondrial potential in *Phytomonas serpens*: electrophoretic Ca(2+) accumulation. Biochim Biophys Acta 2004;1656:96–103.
[45] Fang J, Beattie DS. Identification of a gene encoding a 54 kDa alternative NADH dehydrogenase in *Trypanosoma brucei*. Mol Biochem Parasitol 2003;127:73–77.
[46] Yan L-J, Yang S-H, Shu H, Prokai L, Forster MJ, 2007. Histochemical staining and quantification of dihydrolipoamide dehydrogenase diaphorase activity using blue native PAGE. Electrophoresis 28, 1036–45.
[47] Surve S, Heestand M, Panicucci B, Schnaufer A, Parsons M. Enigmatic presence of mitochondrial complex I in *Trypanosoma brucei* bloodstream forms. Eukaryot Cell 2012;11:183–93.
[48] Morales J, Mogi T, Mineki S, Takashima E, Mineki R, Hirawake H, et al. Novel mitochondrial complex II isolated from Trypanosoma cruzi is composed of 12 peptides including a heterodimeric Ip subunit. J Biol Chem 2009;284:7255–63.
[49] Acestor N, Panigrahi AK, Ogata Y, Anupama A, Stuart KD. Protein composition of *Trypanosoma brucei* mitochondrial membranes. Proteomics 2009;9:5497–508.
[50] Gnipová A, Panicucci B, Paris Z, Verner Z, Horváth A, Lukeš, et al. Disparate phenotypic effects from the knockdown of various *Trypanosoma brucei* cytochrome c oxidase subunits. Mol Biochem Parasitol 2012;184:90–8.
[51] Zíková A, Panigrahi AK, Uboldi AD, Dalley RA, Handman E, Stuart K. Structural and functional association of *Trypanosoma brucei* MIX protein with cytochrome c oxidase complex. Eukaryot Cell 2008;7:1994–2003.
[52] Priest JW, Hajduk SL. Cytochrome c reductase purified from *Crithidia fasciculata* contains an atypical cytochrome c1. J Biol Chem 1992;267:20188–95.
[53] Speijer D, Muijsers AO, Dekker H, de Haan A, Breek CK, Albracht SP, et al. Purification and characterization of cytochrome c oxidase from the insect trypanosomatid *Crithidia fasciculata*. Mol Biochem Parasitol 1996;79:47–59.
[54] Maslov DA, Nawathean P, Scheel J. Partial kinetoplast-mitochondrial gene organization and expression in the respiratory deficient plant trypanosomatid *Phytomonas serpens*. Mol Biochem Parasitol 1999;99:207–21.
[55] Schäfer E, Seelert H, Reifschneider NH, Krause F, Dencher NA, Vonck J. Architecture of active mammalian respiratory chain supercomplexes. J Biol Chem 2006;281:15370–5.
[56] Schägger H, Pfeiffer K. The ratio of oxidative phosphorylation complexes I-V in bovine heart mitochondria and the composition of respiratory chain supercomplexes. J Biol Chem 2001;276:37861–7.
[57] Perotti ME, Anderson WA, Swift H. Quantitative cytochemistry of the diaminobenzidine cytochrome oxidase reaction product in mitochondria of cardiac muscle and pancreas. J Histochem Cytochem 1983;31:351–65.
[58] Verner Z, Paris Z, Lukeš J. Mitochondrial membrane potential-based genome-wide RNAi screen of *Trypanosoma brucei*. Parasitol Res 2010;106:1241–4.
[59] Midgley M, Stephenson MC. Measurement of the membrane potential component of the transmembrane proton electrochemical gradient in *Crithidia fasciculata*. Biochem Soc Trans 1980;8:307–8.
[60] Motta MC, Saraiva EM, Costa e Silva Filho F, de Souza W. Cell surface charge and sugar residues of *Crithidia fasciculata* and Crithidia luciliae. Microbios 1991;68:87–96.
[61] Opperdoes FR, Coombs GH. Metabolism of *Leishmania*: proven and predicted. Trends Parasitol 2007;23:149–58.
[62] Kronick P, Hill GC. Evidence for the functioning of cytochrome o in kinetoplastida. Biochim Biophys Acta: Bioenerg 1974;368:173–80.